Development of a Liquid Chromatography–Electrospray Ionization Tandem Mass Spectrometry Method for Detecting Oxaliplatin–DNA Intrastrand Cross-Links in Biological Samples

ARTICLE *in* CHEMICAL RESEARCH IN TOXICOLOGY · SEPTEMBER 2007

Impact Factor: 3.53 · DOI: 10.1021/tx700088j · Source: PubMed

6 AUTHORS, INCLUDING:

Colin James Henderson
University of Dundee
156 PUBLICATIONS **5,542** CITATIONS
SEE PROFILE

Chris Harrington
Royal Surrey County NHS Foundation Trust
95 PUBLICATIONS **1,481** CITATIONS
SEE PROFILE

Development of a Liquid Chromatography–Electrospray Ionization Tandem Mass Spectrometry Method for Detecting Oxaliplatin–DNA Intrastrand Cross-Links in Biological Samples

Rachel C. Le Pla,*,† Kenneth J. Ritchie,‡ Colin J. Henderson,‡ C. Roland Wolf,‡ Chris F. Harrington,† and Peter B. Farmer†

Cancer Biomarkers and Prevention Group, Biocentre, University of Leicester, University Road, Leicester LE1 7RH, U.K., and Cancer Research UK, Molecular Pharmacology Unit, Biomedical Research Centre, Level 5, Ninewells Hospital and Medical School, Dundee DD1 9SY, U.K.

Received March 22, 2007

Cellular resistance, both intrinsic and acquired, poses a problem in the effectiveness of platinum-based chemotherapy. The cytotoxic activity of Pt-based chemotherapeutic agents is derived from their ability to react with cellular DNA. Oxaliplatin binds to the N7 position of the purine DNA bases, forming mainly intrastrand cross-links between either two adjacent guanines (GG), an adjacent adenine and guanine (AG), or two guanines separated by an unmodified nucleotide (GNG). We report the development of a liquid chromatography–electrospray ionization tandem mass spectrometry (LC–ESI-MS/MS) method for measuring GG and AG intrastrand cross-links formed by oxaliplatin. The limits of detection for GG–oxPt and AG–oxPt were 23 and 19 adducts per 10^8 nucleotides, respectively. We compare the formation and persistence of intrastrand cross-links between wild-type and glutathione transferase P null mice (GSTP null) treated with oxaliplatin. No significant difference was observed in the level of intrastrand cross-links formed by oxaliplatin between the mouse strains in liver, kidney, and lung DNA. Adduct levels were greatest in liver and lowest in lung tissue.

Introduction

Pt-based drugs are among the most effective anticancer agents and have been widely used in the treatment of a variety of tumors. Over the years, a large number of platinum analogues have been synthesised in efforts to overcome resistance and/or reduce the toxicity associated with both the first (e.g., cisplatin) and second generation (e.g., carboplatin) of Pt-based drugs. Oxaliplatin, one of the latest generation of Pt anticancer drugs, has been shown to be active against a broad range of cancers that are known to be intrinsically resistant to cisplatin and carboplatin, including colon, ovarian, cervix, lung, and leukemia (*1*). Oxaliplatin is less toxic than cisplatin and carboplatin, with reduced hematological toxicity, gastrointestinal toxicity, and nephrotoxicity (*1, 2*). Oxaliplatin has been approved for use in the United Kingdom as the first-line therapy for advanced colorectal cancers when used in combination with 5-fluorouracil (5-FU) and folinic acid (FA) (*3*).

Oxaliplatin is an organoplatinum complex in which the platinum atom is complexed with 1,2-diaminocyclohexane (DACH) and with an oxalate ligand as a leaving group. The DACH–Pt complex of oxaliplatin can exist in three isomeric conformations. Kidani et al. (*4*) showed that the *trans*-l(*R*,*R*) isomer of oxaliplatin was the most effective against cisplatin-sensitive and cisplatin-resistant cell lines. Oxaliplatin undergoes nonenzymatic conversion in physiologic solutions to active derivatives via displacement of the labile oxalate ligand. Several transient reactive species are formed, including monoaquo and diaquo DACH platinum, which covalently bind with sulfur and amino groups of proteins and free amino acids, RNA, and DNA.

The antitumor properties of Pt-based drugs are believed to be related to the formation of Pt–DNA adducts. Previous studies with cisplatin have found a good correlation between Pt–DNA adducts and patient therapy outcome (*5–9*). Oxaliplatin primarily forms intrastrand cross-links between the N7 positions of two adjacent guanines (GG), an adenine adjacent to a guanine (AG), and guanines separated by an intervening nucleotide (GNG) (*10*). Oxaliplatin also forms a small proportion of monofunctional adducts, DNA–protein cross-links, and interstrand cross-links (*11*). The cytotoxic efficacy for each of the different types of DNA adducts is as yet unknown. Intrastrand cross-link levels in tumor biopsies taken from patients treated with cisplatin have reported to be approximately 1 per 100 000 and 1 per 300 000 bases for GG and AG intrastrand cross-links, respectively (*12*). Oxaliplatin formed fewer DNA–Pt adducts (as determined by atomic absorption spectroscopy) in cells treated with an equimolar dose of either oxaliplatin or cisplatin (*11*). However, oxaliplatin requires fewer DNA lesions than cisplatin to achieve cell growth inhibition (*11*).

Several mechanisms have been proposed to account for the resistance of some tumors to platinum-based therapies, including an increased level of DNA repair, increased lesion tolerance, defective apoptosis response, a decreased level of intracellular accumulation of the drug, and an increased level of deactivation by intracellular thiol-containing molecules, e.g., glutathione [γ-glutamyl-cysteinyl-glycine (GSH)]. GSH participates in many cellular reactions, including the detoxification of a wide variety of electrophiles which include physiological metabolites and xenobiotics. The conjugation of GSH with an electrophile is catalyzed by the glutathione transferase (GST) family of phase

* To whom correspondence should be addressed: Cancer Biomarkers and Prevention Group, Biocentre, University of Leicester, University Road, Leicester LE1 7RH, U.K. Telephone: +44 (0)116-223-1835. Fax: +44 (0)116-223-1840. E-mail: rclp1@le.ac.uk.

† University of Leicester.

‡ Ninewells Hospital and Medical School.

10.1021/tx700088j CCC: $37.00
Published on Web 07/18/2007

II detoxification enzymes (*13*). GSH-conjugated compounds may then be actively transported out of the cell by the membrane-bound GS-X pump. GSTP encodes a cytosolic GST, GSTπ, which has been associated with resistance to many anti-neoplastic drugs (*14*). GSTP is present in most species as a single gene, GSTP1. However, in mice, there are two GSTP genes, mGSTP1 and mGSTP2 (*15, 16*). mGSTP1 is expressed at much higher levels and is much more catalytically active than mGSTP2 (*17, 18*). In the study presented here, we determine what effect GSTP has on the formation of oxaliplatin–DNA adducts and ultimately the cytotoxicity of oxaliplatin. Toward this end, we compared the level of intrastrand cross-links formed in wild-type and GSTP1/2 null mice treated with oxaliplatin.

Several methods currently exist for the detection and measurement of DNA adducts formed by oxaliplatin, including inductively coupled plasma mass spectrometry (ICP-MS) (*19*), atomic absorption spectroscopy (AAS) (*11*), the COMET assay (*2*), ^{32}P postlabeling (*10*), and adsorptive stripping voltammetry (AdSV) (*20*). With the exception of ^{32}P postlabeling, none of those methods can differentiate between the different types of Pt–DNA damage. Previously, a LC–ESI-MS/MS method was developed for the detection of DNA intrastrand cross-link adducts formed by cisplatin (*21*). We have developed a LC–ESI-MS/MS method suitable for the specific identification and direct measurement of the two major DNA intrastrand cross-link adducts formed by oxaliplatin. This method has been applied to the assessment of oxaliplatin–DNA adducts in wild-type and GSTP1/2 null mice.

Materials and Methods

Materials. 2′-Deoxyadenylyl (3′→5′)-2′-deoxyguanosine (AG) was purchased from biomers.net (Ulm, Germany). Maxi genomic tips and buffers were purchased from Qiagen (Crawley, U.K.). Shrimp alkaline phosphatase (SAP) was purchased from Amersham Life Sciences. All other enzymes and reagents were purchased from Sigma-Aldrich (Poole, U.K.).

Treatment of Calf Thymus DNA with Oxaliplatin. Calf thymus DNA (CT-DNA, 0.5 mg/mL = 1.625 mM dNp) was treated with oxaliplatin between 3.25 nM (1 drug molecule per 5×10^5 dNp molecules) and 16.25 μM (1 drug molecule per 100 dNp molecules) in 6 mL of deionized water for 24 h at 37 °C. DNA was precipitated using 2-propanol (1 volume of isopropanol, 5 min, dry ice) followed by centrifugation (15 000 rpm for 15 min at 4 °C). The supernatant (containing unreacted oxaliplatin) was removed, leaving the DNA pellet. The pellet was washed twice with 2 mL of 2-propanol and resuspended in deionized water to a concentration of 1 mg/mL as determined by UV absorbance spectroscopy.

Treatment of Mice with Oxaliplatin. Three GSTP1/2 knockout and three wild-type male mice on a mixed 129 × MF-1 genetic background were given an intraperitoneal dose of oxaliplatin (10 mg/kg) for 3 days. The mice were sacrificed on the fourth day using an increasing concentration of carbon dioxide. The lung, liver, and kidneys of the mice were removed, snap-frozen in liquid nitrogen, and stored at −80 °C. All animal work was carried out under regulation of the Animal (Scientific Procedures) Act and after local Ethical Review (Ninewells Hospital and Medical School).

Extraction of DNA from Mouse Tissues. DNA was extracted using a Qiagen blood and cell culture kit (Maxi Tip 500/G) as described briefly here. All buffers were provided with the blood and cell culture kit. Tissues were homogenized mechanically using a hand-held glass homogenizer in buffer G2. The homogenate was incubated with RNAse A (200 units) and RNAse T_1 (20 units) at 37 °C for 30 min. The homogenate was then incubated with proteinase K (10 mg) for 1.5 h at 37 °C. The sample was mixed well by vortexing and applied to an equilibrated genomic tip, which was allowed to empty by gravity flow and then washed with 30 mL of buffer QC. DNA was eluted with 15 mL of warm buffer QF (37 °C) and precipitated via the addition of cold 2-propanol (–20 °C, 10.5 mL). The sample was centrifuged (4000 rpm for 25 min at 4 °C) and the supernatant discarded. The DNA pellet was washed twice with 1 mL of 70% ethanol. DNA was resuspended in deionized water and the concentration measured by UV spectrometry at 260 nm.

Scheme 1. Summary of the Sample Preparation Method

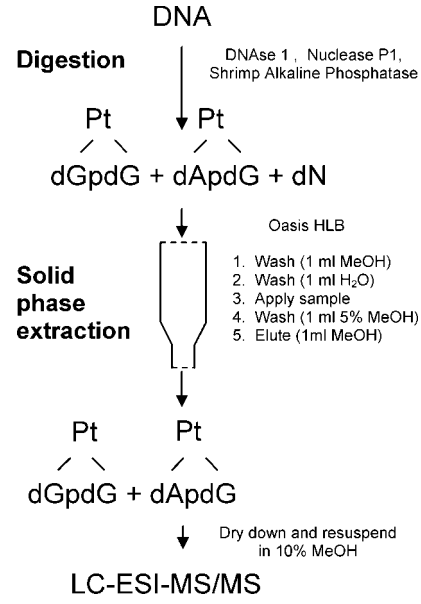

Preparation of Samples for Analysis by LC–ESI-MS/MS. Scheme 1 summarizes the sample preparation method. Samples of DNA (110 μg) were incubated with DNAse I (35.2 units), shrimp alkaline phosphatase (4.4 units), and nuclease P1 (NP1, 8.9 units) in 4 mM $MgCl_2$ and 1 mM $ZnCl_2$ for 6 h at 37 °C (final volume of 240 μL). To each sample was added 760 μL of 5% methanol. Oasis HLB disposable solid phase extraction (SPE) columns (1 cm^3, 30 mg, 30 μm particle size) were used with a SPE vacuum manifold (Phenomenex, Torrence, CA) and a minivacuum pump (XF54 230 50, Millipore, Billerica, MA). The columns were placed in the vacuum manifold, and the vacuum was set to 5 mmHg. Columns were conditioned with 1 mL of methanol, before equilibration with 1 mL of deionized water. Samples were allowed to pass through the column before being washed with 1 mL of 5% methanol. Samples were eluted from the column using 1 mL of methanol and collected in a 2 mL microcentrifuge tube. The samples were dried down in a centrifugal evaporator (Phenomenex) and resuspended in 50 μL of 10% methanol. The samples were transferred to a HPLC vial containing a low-volume insert prior to analysis by LC–ESI-MS/MS.

Preparation of GG– and AG–Oxaliplatin Standards. 2′-Deoxyguanylyl(3′→5′)-2′-deoxyguanosine (GG) (1 mM) or 2′-deoxyadenylyl(3′→5′)-2′-deoxyguanosine (AG) (1 mM) was treated with oxaliplatin (1 mM) in deionized water (final reaction volume of 1 mL) at 37 °C for ∼48 h. The platinated dinucleotides were purified by HPLC using a Supelcosil LC-18 (Supelco UK, Poole, U.K.), 5 μm, 4.6 mm × 250 mm column with a Supelguard guard column (LC-18, 4.0 mm inside diameter) and a KrudKatcher disposable preguard column (5 μm) filter on a Varian Pro Star 210 pump system connected to a Varian Pro Star 320 UV–vis detector set at 254 nm (Varian UK Ltd., Oxford, U.K.). The elution conditions were as follows: solvent A, 1 mM triethylammonium acetate buffer (TEAA) (1:1); solvent B, 100% acetonitrile; flow rate, 0.8 mL/min; gradient, 99% A and 1% B at 0 min, 75% A and 25% B at 120 min, 100% B at 121 min, 100% B at 124 min, 99% A and 1% B at 125 min, and 99% A and 1% B at 130 min. Peaks were collected and characterized by elemental (ICP-MS) and molecular (ESI-MS) mass spectrometry.

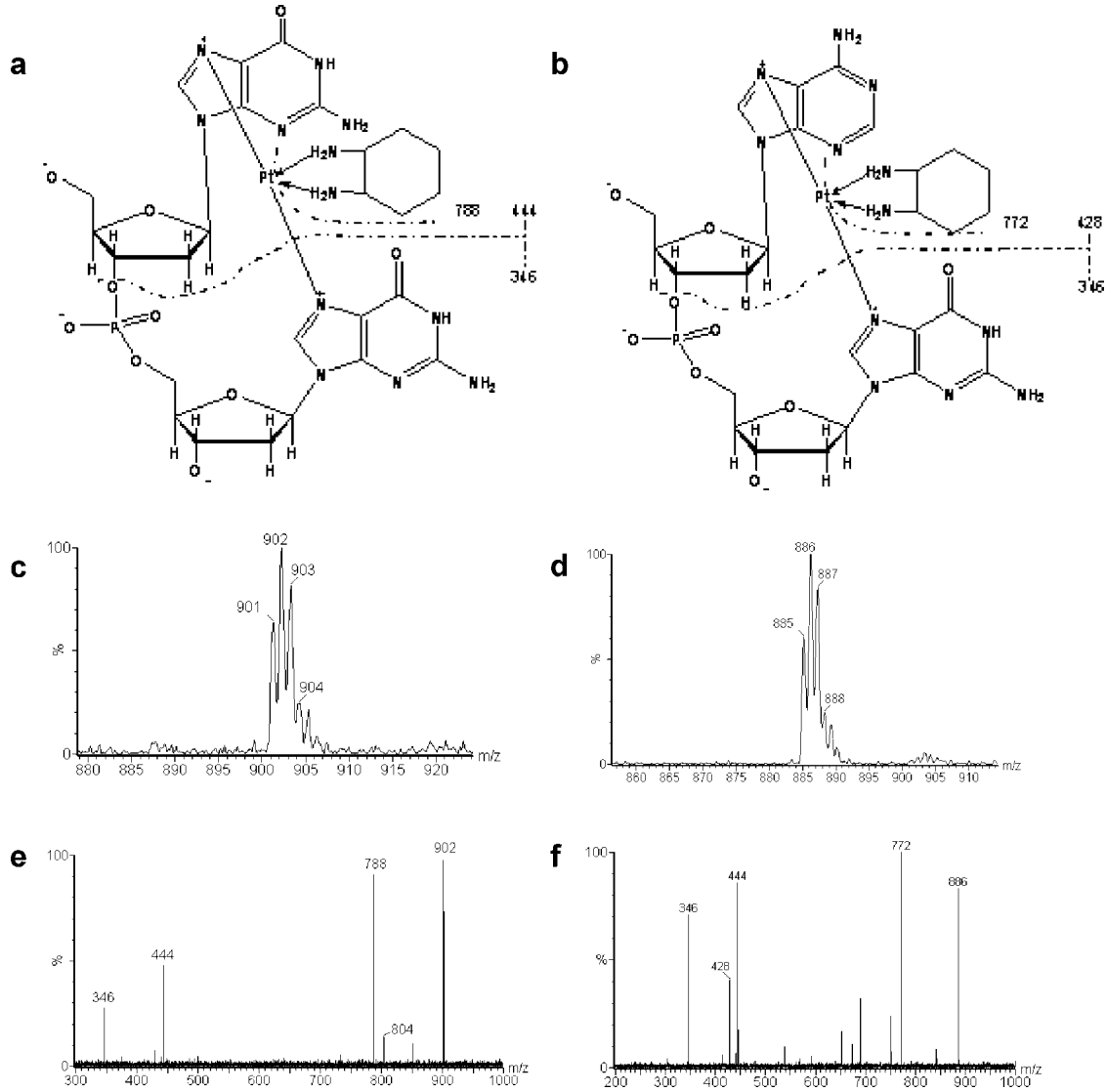

Figure 1. Analysis of GG–oxPt and AG–oxPt by ESI mass spectrometry in negative mode. (a) Structure of the GG–oxPt intrastrand cross-link following enzymatic digestion. (b) Structure of the AG–oxPt intrastrand cross-link following enzymatic digestion. (c) ESI-MS spectrum of the GG–oxPt standard. (d) ESI-MS spectrum of the AG–oxPt standard. (e) ESI-MS/MS product ion spectrum for GG–oxPt (daughters of *m/z* 902; collision energy of 25). (f) ESI-MS/MS product ion spectrum for AG–oxPt (daughters of *m/z* 886; collision energy of 25).

Characterization of GG and AG Platinated Standards. Structural characterization of the two standards was carried out using a Micromass Quattro Ultima (Micromass, Waters Ltd., Manchester, U.K.) tandem quadrupole mass spectrometer with an electrospray (ESI) interface in negative ion mode. The temperature of the electrospray source was maintained at 80 °C and the desolvation temperature at 350 °C. Nitrogen gas was used as the desolvation gas (200 L/h). The cone and capillary voltages were set at 3.20 and 0 kV, respectively. Hex 1 and Hex 2 were set to 1 and 0.5 V, respectively. The aperture was set at 0 V. Ion energies 1 and 2 were both set at 1 (arbitrary unit). The multiplier was set at 750 V. Elution times were as follows: ~25 min for dGpdG [$(M - H)^- = 595$], ~44–48 min for dGpdG–oxPt [~53% yield; $(M - H)^- = 902$], ~30 min for dApdG [$(M - H)^- = 579$], ~49–51 min for dApdG–oxPt [~10% yield; $(M - H)^- = 886$].

The concentration of purified standards was determined by measurement of the total platinum content of the structurally characterized adducts, using inductively coupled mass spectrometry (ICP-MS) (Agilent 7500ce, Agilent Technologies, Manchester, U.K.). The ICP-MS plasma conditions were as follows: forward power, 1550 W; plasma gas, 15 L/min; carrier gas, 0.9 L/min; auxiliary gas, 0.8 L/min. A micromist nebulizer (Glass Expansion) was used with sample delivery via a peristaltic pump. The system was optimized using a 1 ppb tune solution containing Li, Y, Ce, and Tl to give an oxide level of <1.0 % and a doubly charged level of <1.5 %. Indium (500 μg/L) was used as an internal standard and delivered continuously on-line via a T-piece. The method LOD was 1.0 ng/L using the Pt isotopes at *m/z* 194, 195, and 196.

Analysis of Oxaliplatin-Treated DNA Digests by LC–ESI-MS/MS. The LC–ESI-MS/MS system consisted of a Waters Alliance 2695 separations module with a 100 μL injection loop connected to a Micromass Quattro Ultima. Nitrogen gas was used as the desolvation gas (650 L/h) and the cone gas (20 L/h). A 45 μL aliquot of the DNA sample (equivalent to 100 μg of enzymatically digested DNA) was injected onto a Supelcosil LC-18 (250 mm × 2.1 mm, 5 μm) column with a Supelguard LC-18 (2.1 mm inside diameter) guard cartridge and a KrudKatcher disposable precolumn (5 μm) filter. The elution conditions were as follows: solvent A, 5 mM triethylammonium acetate buffer (1:1 equimolar mix of triethylamine and acetic acid); solvent B, 100% methanol; flow rate, 0.15 mL/min; gradient, 90% A and 10% B at 0 min, 45% A and 55% B at 60 min, 90% A and 10% B at 61 min, 90% A and 10% B at 65 min. The collision gas was argon (indicated cell pressure of 2.5×10^{-3} mbar), and the collision energy was set at 30 eV.

The samples were analyzed using multiple-reaction monitoring (MRM) for the $[M - H]^-$ ion to platinated dinucleoside phosphate $[M - C_6H_{14}N_2]^-$ transitions of GG–oxPt (*m/z* 902–788) and for

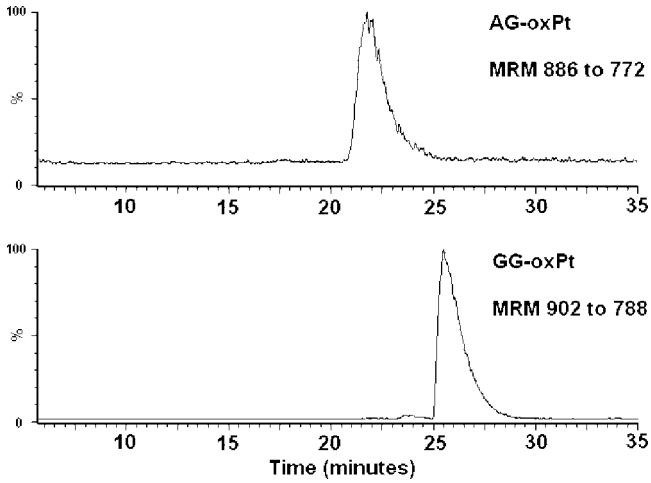

Figure 2. Typical chromatogram obtained for CT-DNA treated with oxaliplatin. Sample separated on a Supelcosil LC-18 column (2.1 mm × 250 mm, 5 μm). Gradient: from 5 mM TEAA and 10% MeOH to 5 mM TEAA and 55% MeOH over 60 min, 150 μL/min. Analyzed with a Micromass Ultima apparatus in negative electrospray mode.

the $[M - H]^-$ ion to platinated dinucleoside phosphate $[M - C_6H_{14}N_2]^-$ transitions of AG–oxPt (*m/z* 886–772). The calibration line was constructed by the addition of different amounts of GG–oxPt and AG–oxPt (ranging from 50 fmol to 50 pmol) to 100 μg of calf thymus DNA for the final amount on the column injected onto the LC–ESI-MS/MS system. The standards were subjected to DNA digestion and the solid phase extraction procedure described above for analysis by LC–ESI-MS/MS.

Statistical Analysis. Data were analyzed using one-way analysis of variance (ANOVA) using Minitab (version 13, Cleocom Ltd., Birmingham, U.K.).

Results

Characterization of GG–oxPt and AG–oxPt Standards by Mass Spectrometry. GG–oxPt and AG–oxPt were synthesised by incubating either GG or AG dinucleoside phosphate with oxaliplatin at 37 °C for 48 h. The adducts were purified by HPLC and analyzed by mass spectrometry as described in Materials and Methods. Panels a and b of Figure 1 show the proposed structures of the GG–oxPt and AG–oxPt dinucleoside phosphate adducts and their major fragments, respectively. Analysis of the platinated adducts by ESI-MS revealed a cluster of peaks, which are primarily due to the multiple isotopes of Pt. The isotope of greatest abundance (^{195}Pt, 33.8%) gives rise to the peaks at 902 and 886 for GG–oxPt and AG–oxPt, respectively (Figure 1c,d). Fragmentation of GG–oxPt and AG–oxPt by ESI-MS/MS primarily resulted in the loss of the 1,2- DACH group (GG–oxPt, *m/z* 902 → 788; AG–oxPt, *m/z* 886 → 772) (Figure 1e,f). Further fragmentation resulted in the production of many additional products, including pdG (*m/z* 346), dG–Pt (*m/z* 444), and dA–Pt (*m/z* 428).

Assessment of GG–oxPt and AG–oxPt in CT-DNA Reacted with Oxaliplatin. CT-DNA was treated with one oxaliplatin molecule per 100–500000 nucleotides for 24 h at 37 °C in deionized water (equivalent to 16.25 μM to 3.25 nM drug). CT-DNA was digested using DNAse I, SAP, and NP1 at 37 °C for 8 h. Salts were removed from the sample by SPE prior to LC–MS/MS analysis (Scheme 1). Recovery of the platinated standards following digestion in the presence of CT-DNA and SPE cleanup was ~95% for GG–oxPt and ~90% for AG–oxPt.

Figure 2 shows a typical LC–ESI-MS/MS MRM ion chromatogram for the assessment of GG–oxPt and AG–oxPt adducts

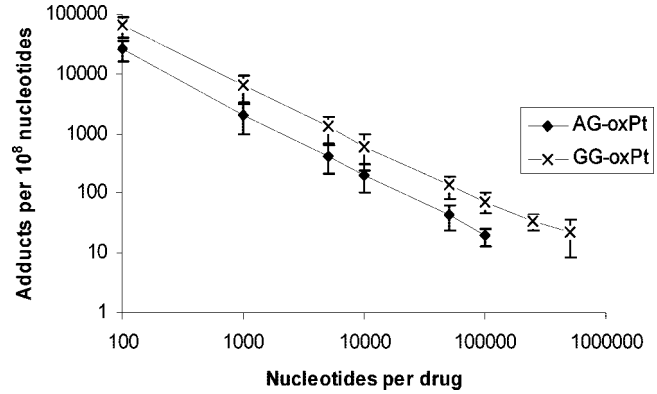

Figure 3. Quantification of GG–oxPt and AG–oxPt adducts in CT-DNA treated in vitro with oxaliplatin with a ratio of one drug molecule per 100–500000 nucleotides (equivalent to 16.25 μM to 3.25 nM). Each dose point represents the average of three independent reactions. Error bars represent ±standard deviation.

in CT-DNA reacted with oxaliplatin. One peak was observed for each of the GG–oxPt and AG–oxPt adducts with retention times of 26 and 22 min, respectively. Figure 3 shows the levels of GG–oxPt and AG–oxPt found at each dose point. The results for each dose point represent the average of three independent reactions each measured three times ($n = 9$). A measurable signal was found for GG–oxPt at all dose points up to and including the sample treated with one oxaliplatin molecule per 5×10^5 nucleotides (CT-DNA treated with one oxaliplatin molecule per 5×10^5 nucleotides contains 22.6 ± 14.1 adducts per 10^8 nucleotides). The method could detect the AG–oxPt adduct in all samples up to and including the sample treated with one oxaliplatin molecule per 10^5 nucleotides (CT-DNA treated with one oxaliplatin molecule per 1×10^5 nucleotides contains 19.4 ± 6.4 adducts per 10^8 nucleotides). No adducts were detected in control samples. The intraday coefficients of variation for GG–oxPt and AG–oxPt were 47.6 and 37.4%, respectively (CT-DNA treated with one oxaliplatin molecule per 5000 nucleotides). The interday coefficients of variation for GG–oxPt and AG–oxPt were 34.6 and 25.7%, respectively (CT-DNA treated with one oxaliplatin molecule per 5000 nucleotides).

Assessment of GG–oxPt and AG–oxPt in DNA Taken from GSTP1/2 Knockout and Wild-Type Mice Treated with 10 mg of Oxaliplatin per Kilogram. Figure 4 shows the mean GG–oxPt levels determined for lung, liver, and kidney DNA obtained from GSTP1/2 null and wild-type mice treated with oxaliplatin (10 mg/kg per day for 3 consecutive days). The LC–ESI-MS/MS method detected GG–oxPt adducts in DNA obtained from lung, liver, and kidneys taken from both GSTP1/2 knockout and wild-type mice treated with oxaliplatin. GG–oxPt levels were slightly higher in the wild-type mice; however, this difference was not significant ($p < 0.05$). Adduct levels were greatest in liver and lowest in lung tissue (liver < kidney < lung). The level of AG–oxPt adducts was close to the limit of detection for the LC–ESI-MS/MS method and could be detected in only a few of the DNA samples. We did not detect any intrastrand cross-links in either the wild-type or GSTP1/2 null mice that were not treated with oxaliplatin.

Discussion

Many of the methods (COMET assay, ICP-MS, AAS, and AdSV) used to measure levels of oxaliplatin–DNA adducts cannot differentiate among the many different types of DNA damage (e.g., intrastand cross-links, interstrand cross-link,

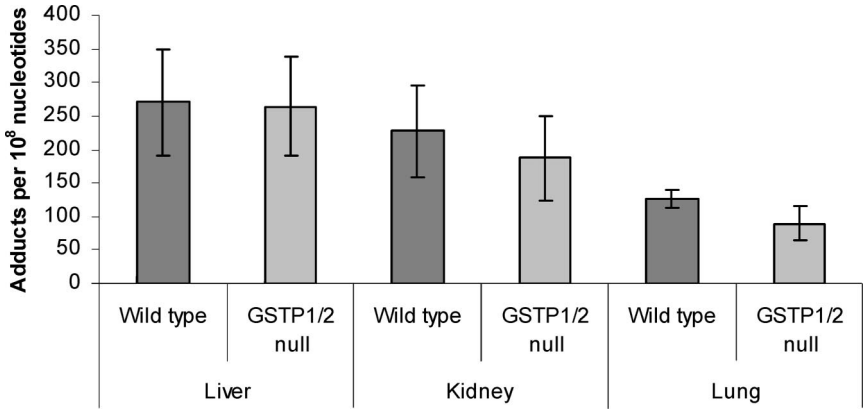

Figure 4. Comparison of GG–oxPt levels in wild-type and GSTP1/2 null mice measured in different tissues ($n = 3$). Each sample was analyzed twice. Error bars represent ±standard deviation.

monofunctional adducts, and DNA–protein cross-links). We have developed a LC–ESI-MS/MS method that is capable of specifically measuring GG and AG oxaliplatin intrastrand cross-link adducts in DNA treated in vitro. The limits of detection for GG–oxPt and AG–oxPt were 23 and 19 adducts per 10^8 nucleotides, respectively (as determined by the analysis of oxaliplatin-treated CT-DNA). This is close to the reported limit of detection of the postlabeling assay reported for cisplatin adducts (10 adducts per 10^8 nucleotides) (*12*). The main advantages of LC–ESI-MS/MS over ^{32}P postlabeling are that it is comparatively quick and easy to prepare samples for analysis (without the use of radiochemicals or NaCN) and it provides some structural information that specifically identifies the adduct being measured (*10, 12*).

More GG–oxPt intrastrand cross-links are formed than AG–oxPt intrastrand cross-links (3.1 ± 0.4 GG–oxPt intrastrand cross-links for every AG–oxPt cross-link formed). The ratio of AG–oxPt to GG–oxPt adducts is consistent with the findings of previous studies (*10*). The method was capable of quantifying GG–oxPt intrastrand cross-links in liver, lung, and kidney samples taken from wild-type and GSTP1/2 null mice treated with oxaliplatin. The level of AG–oxPt intrastrand cross-links in the mice treated with oxaliplatin was extremely close to the limit of detection and could be detected in only a few of the samples. The samples in which AG–oxPt intrastrand cross-links could be detected were split equally between the wild-type and GSTP1/2 null groups. The method did not detect any intrastrand cross-links in untreated mice (wild-type and GSTP1/2 null).

Previously, it was suggested that GSTP1 may play an important role in the detoxification of Pt anticancer compounds, removing the drug before it can react with the DNA. GSTP1 activity has been found to be elevated in some drug-resistant tumors (*21*). In humans, a single nucleotide substitution at position 313 of the GSTP1 gene, which results in the replacement of isoleucine with valine, substantially diminishes GSTP1 activity. Patients who are homozygous for this polymorphism have been shown to respond better to 5-fluorouracil/oxaliplatin therapy (*21*). In addition to catalyzing the conjugation of various electrophiles to glutathione, GSTP1 plays an important role in cellular signaling in response to cellular stress. GSTP1 has been shown to bind to the C-terminus of Jun N-terminal kinase (JNK), preventing it from phosphorylating c-jun which in turn activates a battery of genes involved in apoptosis and cytoprotection (*22, 23, 16*). Ishii et al. (*24*) found that depletion of GSTP1 by antisense expression led to increased levels of apoptosis and necrosis. Patients who have reduced GSTP1 activity may also be more susceptible to the toxic side effects of Pt drugs. Initial studies into the toxicity of cisplatin in the GSTP1/2 null mouse model showed that treatment resulted in greater weight loss and increased liver and kidney damage in mice lacking GSTP (*16*). However, in this study, we did not observe any significant difference in toxicity between the GSTP1/2 null and wild-type mice treated with oxaliplatin using the developed method. We found that there was no significant difference in the level of GG–oxPt adducts found in wild-type and GSTP1/2 null mice in any of the organs that were tested ($p > 0.05$). It is possible that a significant difference between wild-type and GSTP1/2 null mice could have been observed in lung tissue if the number of animals used in this study had been greater.

Conclusion

The cytotoxic activity of Pt-based chemotherapeutic agents is derived from their ability to react with cellular DNA. We have developed a LC–ESI-MS/MS method capable of specifically detecting and quantifying GG–oxPt and AG–oxPt intrastrand cross-links. Using this method, we found that there was no significant difference between the level of GG–oxPt intrastrand cross-links found in GSTP1/2 null and wild-type mice.

Acknowledgment. This work was supported by Medical Research Council, U.K. (Grant G0100873), awarded to P.B.F. and a Cancer Research Programme Grant awarded to C.R.W. The authors of this paper are partners of ECNIS (Environmental Cancer Risk, Nutrition and Individual Susceptibility), a network of excellence operating within the European Union 6th Framework Program, Priority 5: "Food Quality and Safety" (Contract 513943). The ICP-MS instrument purchase was supported by the BBSRC REI initiative (Grant BB/D524416/1).

References

(1) Raymond, E., Faivre, S., Chaney, S., Woynarowski, J., and Cvitkovic, E. (2002) Cellular and molecular pharmacology of oxaliplatin. *Mol. Cancer Ther. 1*, 227–235.

(2) Almeida, G. M., Duarte, T. L., Steward, W. P., and Jones, G. D. D. (2006) Detection of oxaliplatin-induced DNA crosslinks in vitro and in cancer patients using the alkaline comet assay. *DNA Repair 5*, 219–225.

(3) National Institute for Health and Clinical Excellence (NICE) (2005) Irinotecan, oxaliplatin and raltitrexed for the treatment of advanced colorectal cancer. Technology Appraisal 93, NICE, London.

(4) Kidani, Y., Inagaki, K., Iigo, M., Hoshi, A., and Kuretani, K. (1978) Anti-tumor Activity of 1,2-Diaminocyclohexane-Platinum Complexes Against Sarcoma-180 Ascite Form. *J. Med. Chem. 21*, 1315–1318.

(5) Reed, E., Yuspa, S. H., Zwelling, L. A., Ozols, R. F., and Poirier, M. C. (1986) Quantitation of cis-diamminedichloroplatinum II (cisplatin)-DNA intrastrand adducts in testicular and ovarian cancer patients receiving cisplatin chemotherapy. *J. Clin. Invest. 77*, 545–550.

(6) Reed, E., Ozols, R. F., Tarone, R., Yuspa, S. H., and Poirier, M. C. (1987) Platinum DNA adducts in leukcocyte DNA correlates with disease response in ovarian cancer patients receiving platinum based chemotherapy. *Proc. Natl. Acad. Sci. U.S.A. 84*, 5024–5028.

(7) Reed, E., Ozols, R. F., Tarone, R., Yuspa, S. H., and Poirier, M. C. (1988) The measurement of cisplatin-DNA adduct levels in testicular cancer patients. *Carcinogenesis 9*, 1909–1911.

(8) Gupta-Birt, S., Shamkhani, H., Reed, E., Tarone, R. E., Allegra, C. J., Pai, L. H., and Poirier, M. C. (1993) Relationship between patient response in ovarian and breast cancer and platinum drug-DNA adduct formation. *Cancer Epidemiol., Biomarkers Prev. 2*, 229–234.

(9) Parker, R. J., Gill, I., Tarone, R., Vionnet, J. A., Grunberg, S., Muggia, F. M., and Reed, E. (1991) Platinum-DNA damage in leukocyte DNA of patients receiving carboplatin and cisplatin chemotherapy, measured by atomic absorption spectrometry. *Carcinogenesis 12*, 1253–1258.

(10) Saris, C. P., van de Vaart, P. J. M., Rietbroek, R. C., and Blommaert, F. A. (1996) In vitro formation of DNA adducts by cisplatin, lobaplatin and oxaliplatin in calf thymus DNA in solution and in cultured human cells. *Carcinogenesis 17*, 2763–2769.

(11) Woynarowski, J. M., Faivre, S., Herzig, M. C. S., Arnett, B., Chapman, W. G., Trevino, A. V., Raymond, E., Chaney, S. G., Vaisman, A., Varchenko, M., and Juniewicz, P. E. (2000) Oxaliplatin-induced damage of cellular DNA. *Mol. Pharmacol. 58*, 920–927.

(12) Welters, M. J. P., Maliepaard, M., Jacobs-Bergmans, A. J., Baan, R. A., Schellens, J. H. M., Ma, J. G., van der Vijgh, W. J. F., Braakhuis, B. J. M., and Fichtinger-Schepman, A. M. J. (1997) Improved P-32 postlabelling assay for the quantification of the major platinum-DNA adducts. *Carcinogenesis 18*, 1767–1774.

(13) Wu, G.Y., Fang, Y. Z., Yang, S., Lupton, J. R., and Turner, N. D. (2004) Glutathione metabolism and its implications for health. *J. Nutr. 134*, 489–492.

(14) Yang, P., Ebbert, J. O., Sun, Z., and Weinshilboum, R. M. (2006) Role of the Glutathione Metabolic Pathway in Lung Cancer Treatment and Prognosis: A Review. *J. Clin. Oncol. 24*, 1761–1769.

(15) Bammler, T. K., Smith, C. A. D., and Wolf, C. R. (1994) Isolation and Characterization of 2 mouse Pi-class Glutathion-S-Transferase Genes. *Biochem. J. 298*, 385–390.

(16) Henderson, C. J., and Wolf, C. R. (2005) Disruption of the glutathione transferase Pi class genes. *Methods Enzymol. 401*, 116–135.

(17) Bammler, T. K., Driessen, H., Finnstrom, N., and Wolf, C. R. (1995) Amino acid differences at Position 10, Position 11 and Position 104 explain the profound differences between 2 Murine Pi class Glutathione-S-Transferases. *Biochemistry 34*, 9000–9008.

(18) McLellan, L. I., and Hayes, J. D. (1987) Sex-specific constitutive expression of the preneoplastic marker Glutathione-S-Transferase, YFYF, in mouse liver. *Biochem. J. 245*, 399–406.

(19) Ta, L., Espeset, L., Podratz, J., and Windebank, A. J. (2006) Neurotoxicity of oxaliplatin and cisplatin for dorsal root ganglion neurons correlates with platinum-DNA binding. *Neurotoxicology 27*, 992–1002.

(20) Weber, G., Messerschmidt, J., Pieck, A. C., Junker, A. M., Wehmeier, A., and Jaehde, U. (2004) Ultratrace voltammetric determination of DNA-bound platinum in patients after administration of oxaliplatin. *Anal. Bioanal. Chem. 380*, 54–58.

(21) Iijima, H., Patrzyc, H. B., Dawidzik, J. B., Budzinski, E. E., Cheng, H. C., Freund, H. G., and Box, H. C. (2004) Measurement of DNA adducts in cells exposed to cisplatin. *Anal. Biochem. 333*, 65–71.

(22) Stoehlmacher, J., Park, D. J., Zhang, W., Groshen, S., Tsao-Wei, D. D., Yu, M. C., and Lenz, H. J. (2002) Association between glutathione S-transferase P1, T1, and M1 genetic polymorphism and survival of patients with metastatic colorectal cancer. *J. Natl. Cancer Inst. 94*, 936–942.

(23) Adler, V., Yin, Z. M., Fuchs, S. Y., Benezra, M., Rosario, L., Tew, K. D., Pincus, M. R., Sardana, M., Henderson, C. J., Wolf, C. R., Davis, R. J., and Ronai, Z. (1999) Regulation of JNK signalling by GSTp. *EMBO J. 18*, 1321–1334.

(24) Wang, T., Arifoglu, P., Ronai, Z., and Tew, K. D. (2001) Glutathione S-transferase P1-1 (GSTP1-1) inhibits c-Jun N-terminal kinase (JNK1) signaling through interaction with the C terminus. *J. Biol. Chem. 276*, 20999–21003.

(25) Ishii, T., Fujishiro, M., Masuda, M., Nakajima, J., Teramoto, S., Ouchi, Y., and Matsuse, T. (2003) Depletion of glutathione S-transferase P1 induces apoptosis in human lung fibroblasts. *Exp. Lung Res. 29*, 523–536.

TX700088J